Photoelectrochemistry of Films of Quantum Size Lead Sulfide Particles Incorporated in Self-Assembled Monolayers on Gold

Shuichiro Ogawa, Kai Hu, Fu-Ren F. Fan, and Allen J. Bard*

Department of Chemistry and Biochemistry, The University of Texas at Austin, Austin, Texas 78712

Received: February 26, 1997[⊗]

Films of AOT-capped (AOT = dioctyl sulfosuccinate) lead sulfide nanoparticles (Q-PbS) were prepared by incorporation into a self-assembled monolayer of hexanethiol on Au. The Q-PbS particles showed either cathodic or anodic photocurrents, depending on the existence of a hole scavenger or an electron scavenger in the contacting solution, on the state of the surface, and on the electrode potential. The electrochemistry of Q-PbS indicated that the anodic dissolution of Q-PbS occurred at about 0.25 V vs SCE and was not particle size dependent, while the cathodic corrosion potentials of Q-PbS ranged from −1.1 V vs SCE to beyond the hydrogen evolution potential and depended on the size of the Q-PbS particles.

Introduction

Lead sulfide has been used in several applications, e.g., an IR detector,[1] a solar absorber,[2] Pb^{2+} ion-selective sensors,[3] and photography.[4] Because bulk PbS is a black material with a small band gap (0.41 eV at 298 K),[5] it has not been investigated in photoelectrochemical cells (e.g., photovoltaic cells for solar energy conversion). A solar thermophotovoltaic converter[6] using PbS has been reported, however. PbS thin films can be produced by several processes, such as electrochemical deposition[7] and chemical bath deposition.[8]

Davis and Huang[9] have studied the electrochemical oxidation of PbS by using a rotating ring−PbS disk electrode. The major oxidation reaction, observed at 0.2−0.3 V vs SCE, was

$$PbS(s) \rightarrow Pb^{2+} + S(s) + 2e^- \quad (1)$$

which was independent of pH in the presence of oxygen. The standard electrode potential calculated for this reaction is 0.144 V vs SCE.[10] The anodic dissolution of the ore galena, the major component of which is PbS, has also been investigated,[11] and these studies suggest oxidation occurs via eq 1.

In this paper we investigate the possibility of using quantum-size (Q-) particles of PbS with larger band gaps than the bulk material in photoelectrochemical cells. Methods of preparation, characterization, and the effect of particle size on the material properties of Q-PbS have been investigated.[12] Nenadovic et al.[13] estimated the position of the lowest empty electronic state in 4 nm Q-PbS particles to be about −0.1 eV vs SCE in 0.1 M 2-propanol by establishing the position of equilibrium between viologen radicals and the Q-PbS particles. Yoneyama and co-workers[14−16] found that the different surface structures obtained by changing the relative concentration of Pb^{2+} and S^{2-} ions in the synthesis of PbS particles greatly affected the photochemical and photoelectrochemical properties in capped PbS particles.[14] They also found that the photoinduced reduction of methyl viologen[17] on Q-PbS particles modified with 4-aminothiophenol was influenced by both the pH of the solution and the type of hole scavenger.[15] They also indicated that the onset potential for anodic photocurrent at Nafion-coated electrodes with incorporated Q-PbS shifted negative with an increase in band gap.[16]

In this study, films of Q-PbS particles incorporated in a self-assembled monolayer (SAM) on gold were prepared (Scheme 1) and the electrochemical and photoelectrochemical properties of the films were investigated.

SCHEME 1: Schematic Diagram of the Q-PbS Particle Film

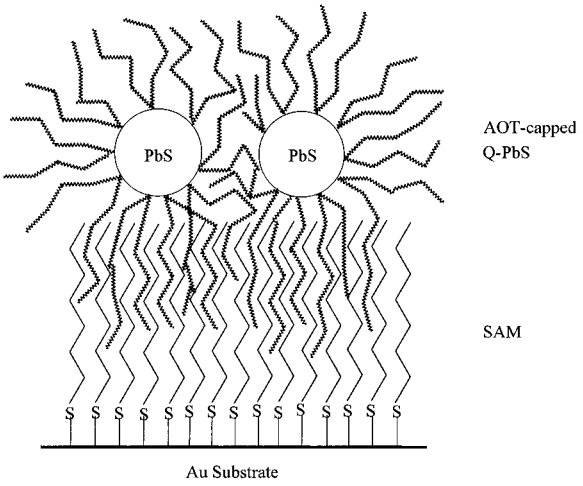

Experimental Section

Chemicals and Materials. High-purity water (Millipore >18 MΩ·cm) was used in the preparation of all solutions. All chemicals were reagent or spectrographic grade and were used as received: 0.5 M $NaClO_4$ (Fisher Scientific, Fair Lawn, NJ) as supporting electrolyte, $Na_2S_2O_4$ (Eastman Organic Chemicals, Rochester, NY), sulfur powder (Mallinckrodt Inc., Paris, KY), methyl viologen dichloride hydrate ($MVCl_2$; Aldrich, Milwaukee, WI), benzoquinone (Matheson, Norwood, OH). All of the solutions were deoxygenated with argon.

Preparation of Q-PbS Particles. Lead sulfide particles were prepared in inverse micelles following the method of Steigerwald et al.[18] for cadmium sulfide particles. Typically two separate solutions, both containing 125 mL of spectrographic grade heptane (Fisher) and 11.1 g of dioctyl sulfosuccinate (AOT; Aldrich) were prepared under argon. To one solution (A), 0.88 mL of an aqueous solution of 1.8 M $Pb(ClO_4)_2 \cdot 6H_2O$ (Alfa, Ward Hill, MA) was added. To the other solution (B), 0.88 mL of a deoxygenated aqueous solution of 0.6 M $Na_2S \cdot 9H_2O$ (EM Science, Gibbstown, NJ) was added. Both

[⊗] Abstract published in *Advance ACS Abstracts,* July 1, 1997.

S1089-5647(97)00737-2 CCC: $14.00

solutions were stirred vigorously for 4 h. Solution A was then added dropwise to solution B under argon in the dark within 45 min, and this mixture was stirred under argon in the dark for l h. The resulting solution appeared clear and colorless with some scattered black precipitates (larger PbS particles) on the walls of the container. Different PbS particle sizes were obtained by sampling portions of the upper clear solution after different lengths of time (immediately to 60 days).

Preparation of Gold Substrates. The gold substrates were prepared by sputtering gold (~200 nm thick) on freshly cleaved mica. Before use, the gold surfaces were cleaned with hot chromic acid solution (saturated $K_2Cr_2O_7$ (Fisher) in 90% H_2SO_4 (EM Science)) for 30−60 s and then rinsed with copious amounts of water. This process was repeated until the surface contact angle between water and the gold surface was less than 20° (typically between 8° and 16°), indicating that the gold surface was clean.

Preparation of Dithiol Monolayers on Gold. A 5 mM hexanedithiol (Aldrich) solution was prepared in ethanol (Absolute, Midwest Grain Products, Perkin, IL). SAMs were prepared by immersing the gold substrates in this solution for 10−20 h. After immersion, the samples were removed from solution, rinsed with EtOH at least 3 times and then dried with a stream of argon.

Preparation of Q-PbS Particle Layers. Q-PbS particle layers were prepared by immersing the SAM-covered Au substrate in the heptane solution containing the Q-PbS particles described above for 10−20 h. The samples were then rinsed with heptane several times and dried with argon. The samples were stored in the dark under vacuum.

Preparation of PbS Thin Films. The polycrystalline PbS thin films on indium tin oxide were prepared by chemical bath deposition.[8] The thickness of these films was about 100 nm.

Apparatus. The Teflon cell for photoelectrochemical studies was designed to prevent exposure of the edges of the working electrodes to the solution (see Figure 1 of ref 19). The working electrode contacted the solution through a hole in the side wall of the cell and was sealed against the wall with an O-ring, which defined the area exposed to the solution as 0.3 cm^2. A sheet of Plexiglas held by two screws secured the working electrode in the cell wall. The quartz window was similarly sealed through a larger hole in the opposite wall of the cell. A saturated calomel reference electrode (SCE) and a platinum sheet counter electrode were used for all measurements. The deoxygenated solution contained 0.5 M Na_2SO_4 as the supporting electrolyte and was unbuffered. Before each series of measurements, the Teflon cell and counter and reference electrodes were cleaned with a HNO_3 solution to prevent contamination. The photoelectrochemical system is shown schematically in Figure 2 of ref 19. The electrodes were irradiated through a 17-cm water bath with a tungsten−halogen lamp (type 250-T40-CL, Sylvania Electric Products, Fall River, MA) operated to produce an intensity of 5.5 mW/cm^2 at the electrode position. The power of the lamp was determined with a radiometer/photometer (Model 550-1, Princeton Applied Research (PAR), Princeton, NJ). Photocurrents were detected with a lock-in amplifier (time constant, 1−3 s) with the light chopped at a frequency of 50 Hz. This removed any interference from any dark current that might flow at a given potential. A potentiostat (Model 173, PAR), a universal programmer (Model 175, PAR), a lock-in amplifier (Model 5210, PAR), a variable frequency light chopper (Model 192, PAR), and an X-Y_1Y_2 recorder (Soltec, Sun Valley, CA) were used in these experiments. Absorption spectra were obtained with a Spectronic 3000 array spectrophotometer (Milton Roy Company, Urbana, IL).

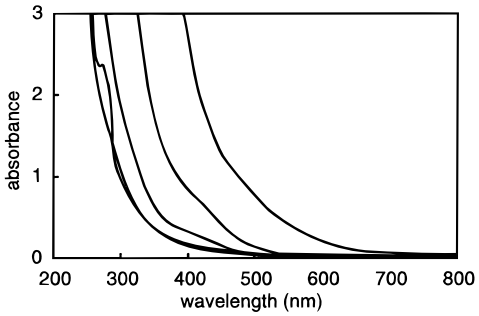

Figure 1. (a) Absorption spectra of the Q-PbS particles in heptane solutions. The absorption curves represent solutions separated from the mother solution after lengths of time corresponding to, from left to right, immediately after preparation and 3, 7, 15, and 60 days. The diameters of the Q-PbS particles were determined from the absorption maximum and the absorption edge[12c] to be about, from left to right, <1.2, 1.3, 1.9, 2.5, and 4.2 nm. The absorption edge of bulk PbS is 3020 nm.

Results and Discussion

Absorption Spectra. Typical absorption spectra of Q-PbS particles in heptane solution obtained by sampling portions of upper clear solution from the original particle preparation after different lengths of time are shown in Figure 1. The sizes of the Q-PbS particles were determined by the absorption maximum and the absorption edge of the spectrum and the data of Wang et al.[12c] These Q-PbS particle solutions, sampled at different times, showed various colors: colorless (immediately after preparation), light yellow (3 days), yellow (7 days), orange (15 days), and brown (60 days). The sizes of these different colored Q-PbS particles in solution are in good agreement with those prepared in Nafion by Miyoshi et al.[16]

Generally, the Q-particle size can be controlled by the ratio $[H_2O]/[AOT]$ in solution. However, in our case, attempts to control the Q-PbS particle size in this way were not successful. We noted that Q-PbS particles within the original preparation (mother) solution grew much faster than those in solution samples separated from the mother solution, although the size of the latter Q-PbS particles also increased after a long time (3 months). The reason for the faster growth rate of the Q-PbS particles within the mother solution is not clear. The only obvious difference between the mother solution and the separated one is that the former has some scattered black particles on the wall of the container. These scattered precipitates, and perhaps smaller unobserved ones, may serve as nucleation centers which the Q-PbS particles in the solution may adsorb on and later desorb from. In this way, the particles within the mother solution may grow faster than those in separated solutions where no nucleation centers are present. The larger precipitates might also decompose into smaller particles which then desorb and diffuse into solution.

Electrochemistry in the Dark. Figure 2a shows the first cyclic voltammogram for 4.2 nm Q-PbS particles by scanning the potential in the positive direction from 0 V vs SCE in a solution of 0.5 M $NaClO_4$ (pH 6.7) with no additional redox species. Significant anodic current is observed at about 0.25 V, due to the oxidative dissolution of PbS (eq 1). This anodic current is attributed to the oxidation of the Q-PbS particles. After the first scan to 0.4 V, additional scans produced essentially no current in this region. The total charge collected during the anodic process corresponded well with the amount of PbS deposited on the gold substrate, assuming that the dissolution reaction is a two-electron process. For other Q-PbS particle sizes, all cyclic voltammograms showed anodic peak currents at essentially the same potential with different magnitudes, indicating that the anodic dissolution process did not depend on the particle size.

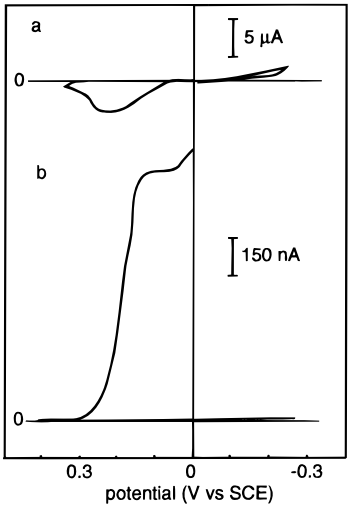

Figure 2. (a) Dark current and (b) photocurrent vs potential curves of a Q-PbS particle layer in a solution containing only 0.5 M $NaClO_4$. The potential range was between 0.4 and −0.3 V; sweep direction was 0 → 0.42 → −0.28 V. Potential scan rate was 5 mV/s. Light intensity was 5.5 mW/cm^2. A lock-in amplifier with a 50 Hz chopping frequency and 1 s time constant was used to detect the photocurrent.

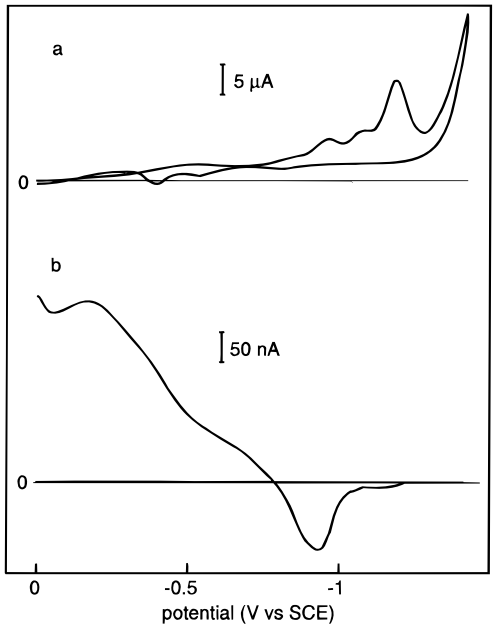

Figure 3. (a) Dark current and (b) photocurrent vs potential curves of a Q-PbS particle layer in a solution containing only 0.5 M $NaClO_4$. The potential range was between 0 and −1.4 V; sweep direction was 0 → −1.4 → 0 V. The other experimental conditions were the same as those in Figure 2.

Figure 3a shows the first cyclic voltammogram for scanning a 4.2 nm Q-PbS particle layer in the negative direction from 0 V vs SCE. If the potential was reversed at around −0.7 V, the anodic peaks at −0.4 and −0.55 V were not observed. If the potential was reversed at about −1.0 V, just past the peak at −0.97 V, anodic peaks appeared at −0.55 and −0.8 V. If the potential was reversed at about −1.1. V, no new peaks appeared in the reverse anodic scan. If the potential was reversed at about −1.25 V, an anodic peak appeared at about −0.4 V. Under illumination, a photocurrent could be continuously observed if the potential was held positive of −1.1 V; however, it disappeared once the potential was scanned beyond the peak at −1.2 to −1.3 V, suggesting that the reduced products of Q-PbS were not photoelectrochemically active. One possible process that would account for the reduction peak at about −1.2 V and the reoxidation peak at −0.4 V is the reduction of Q-PbS to Pb and the reoxidation of Pb to Pb^{2+}. This oxidation process was confirmed by the deposition and stripping of Pb on the electrode in the presence of a small amount of added $Pb(ClO_4)_2$ solution.

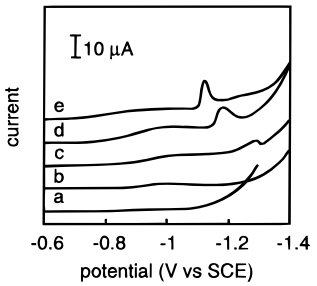

Figure 4. Dark current vs potential curves for (a) clean Au and (b) 1.3, (c) 1.9, (d) 2.5, and (e) 4.2 nm PbS particle layers.

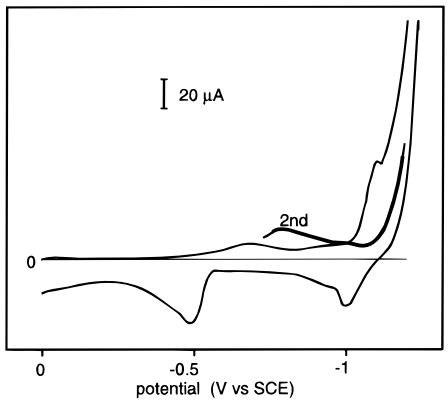

Figure 5. Dark current vs potential curves of a bulk PbS thin layer. The potential range was between 0 and −1.25 V; sweep direction was 0 → −1.25 → 0 V. The thicker line represents the second scan.

The dark cathodic current−potential curves of Q-PbS films of different particle sizes are given in Figure 4. Clearly, the reduction peak potential is particle size dependent. For the reduction of a 1.3 nm Q-PbS particle layer (Figure 4b), there was no clear reduction peak before hydrogen evolution, which in all cases is shifted to more negative potentials by the PbS particle layer on Au. In the return scan, the anodic current at about −0.4 V was not detected, suggesting that the cathodic corrosion process of Q-PbS of this size was beyond hydrogen evolution in this electrolyte. The reduction curves for 1.9, 2.5, and 4.2 nm Q-PbS particle films (Figure 4c−e) show reduction peak potentials at about −1.3, −1.2, and −1.1 V vs SCE, respectively. Anodic peaks around −0.4 V were observed for all these curves in the reverse anodic scans (not shown). All of these reduction peaks disappeared on a second cathodic scan, suggesting that the original reduction peaks around −1.2 V indeed represented the irreversible reduction of the Q-PbS particles. The particle size dependence of the reduction potential could be attributed to the quantum size effect. As the Q-PbS particle size decreased, its band-gap energy increased, moving the conduction band position to a more negative potential. This band-gap increase thus makes it more difficult to add electrons into the conduction band, presumably the initial step in PbS reduction. Further investigation of the relationship between electrochemical redox potential and semiconductor band-gap energy is of interest.

Figure 5 shows the voltammetric curves of a bulk PbS thin film in the dark. The reduction peak at −1.1 V, as discussed above, is associated with cathodic corrosion, because after sweeping the potential back to 0 V, no photocurrent was observed, and this peak did not appear in the second scan. This potential is consistent with the cathodic corrosion potential of PbS reported by Nenadovic et al.[13]

From these electrochemical and photoelectrochemical measurements, we conclude that the anodic dissolution potential of

SCHEME 2: Schematic Energy Diagrams of the Interface between the Electrolyte and Q-PbS Particle Layer in a Solution with No Redox Species[a]

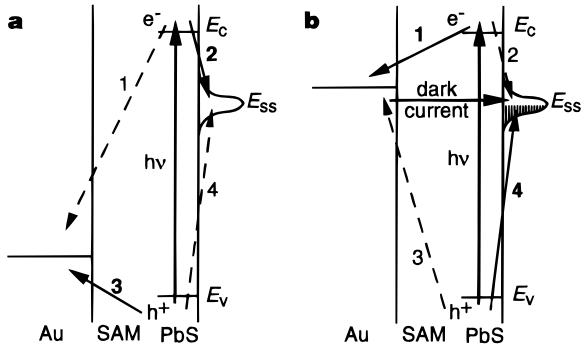

[a] E_c = conduction band energy, E_{ss} = surface state energy, and E_v = valence band energy. (a) With the potential of the Q-PbS layer held at 0 V vs SCE, processes 2 and 3 are dominant. (b) With the potential of the Q-PbS layer held at about −1.0 V vs SCE, processes 1 and 4 are dominant.

Q-PbS is around 0.25 V vs SCE, which is almost the same as that of bulk PbS. Electrochemical studies on bulk PbS have been reported,[11] and several redox reactions have been suggested.[12] We did not carry out additional electrochemical studies to elucidate the processes during voltammetry.

Photoelectrochemistry. In a solution containing only supporting electrolyte, a cathodic photocurrent of the order of 50 nA was observed when the Q-PbS layer was held at 0 V vs SCE. Although the photocurrent was fairly stable for a period of over 1 h, it decayed slowly with time, indicating a slow reductive degradation of the PbS layer. A schematic diagram of the proposed process is given in Scheme 2a, where the level shown as a surface state is presumably initially a Pb(II) state. However, as shown in Figure 2, if the electrode was held initially at 0 V vs SCE and then scanned to more positive potentials (0.4 V), the current decayed to background, and neither photocurrent nor dark current was observed following a sweep toward more negative potentials, presumably because the anodic dissolution of the Q-PbS particles occurred. Thus at 0 V the cathodic photocurrent mainly causes filling of the initially vacant surface states (process 2 in Scheme 2a) and slow reduction of the Q-PbS.

When the applied potential was made more negative (e.g., −1.0 V vs SCE) so that the surface states are initially filled (partial reduction of the Q-PbS), these states act as electron donors (hole acceptors) for the photogenerated holes (process 4 in Scheme 2b) and an anodic photocurrent is observed (Figure 3). This anodic photocurrent is partially compensated by the cathodic dark current that flows in this potential region. Note that although in Schemes 2 and 3 only a single surface state is shown, the dark voltammetric curves as in Figure 3a show several cathodic current peaks between −0.2 and −1.2 V, each of these presumably representing a reductive process associated with a different particle vacant energy level.

The proposed mechanism of the photoelectrochemical behavior of these particles differs from that usually found with bulk (e.g., single crystal) semiconductors, where the photocurrent is predominantly cathodic (p-type) or anodic (n-type). Whereas in bulk semiconductors the direction of flow of photogenerated charge carriers is mainly determined by the field (band-bending) in the space charge region, in Q-particles this field is unimportant, and current direction is governed by the availability of vacant or filled states at the energy appropriate to the applied potential. To investigate this bidirectional photocurrent flow further and also decrease the rate of cathodic and anodic degradation of the Q-PbS particles under irradiation,

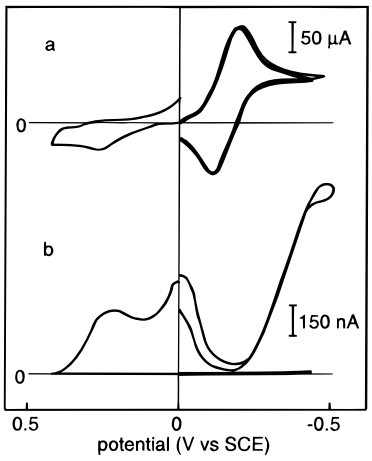

Figure 6. (a) Dark current and (b) photocurrent vs potential curves of a Q-PbS particle layer in a solution containing 10 mM benzoquinone and 0.5 M $NaClO_4$. The potential range was between 0.4 and −0.5 V; sweep direction was 0 → −0.5 → 0.4 → −0.5 → 0 V. The other experimental conditions were the same as those in Figure 2. The thicker lines represent the last scan between 0 and −0.5 V.

SCHEME 3: Schematic Energy Diagrams of the Interface between the Electrolyte and Q-PbS Particle Layer in Solutions Containing (a) Benzoquinone (BQ), (b) the Reduced Form of Methyl Viologen ($MV^{\bullet+}$), and (c, d) Polysulfide[a]

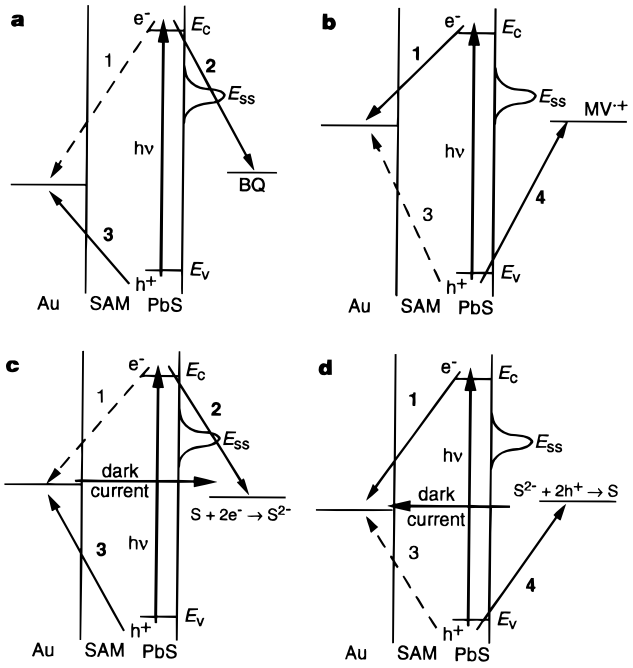

[a] (a) With BQ as an electron scavenger, processes 2 and 3 are dominant. (b) With $MV^{\bullet+}$ as a hole scavenger, processes 1 and 4 are dominant. (c) With S_x^{2-} as an electron scavenger, processes 2 and 3 are dominant. (d) With S_x^{2-} as a hole scavenger, processes 1 and 4 are dominant.

experiments in which mediators (either electron acceptors or donors) were added to the solution were undertaken.

Figure 6 shows the voltammetric curves obtained under illumination in a solution (pH 6.6) containing 10 mM benzoquinone as an electron scavenger. The enhanced cathodic photocurrent at potentials negative of −0.3 V may be attributed to the photoreduction of benzoquinone by the photogenerated electrons via the conduction band or surface states (Scheme 3a). Opposite behavior is found when an electron donor is used as a mediator. Figure 7 shows the voltammetric curves obtained under illumination in a solution (pH 5.3) containing 2 mM $MV^{\bullet+}$ (methyl viologen reduced by $Na_2S_2O_4$) as a hole scavenger. The

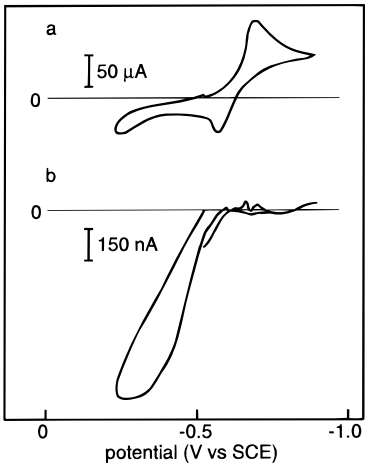

Figure 7. (a) Dark current and (b) photocurrent vs potential curves of a Q-PbS particle layer in a solution containing 2 mM $MV^{\bullet+}$ and 0.5 M $NaClO_4$. The potential range was between −0.23 and −0.9 V; sweep direction was −0.52 → −0.9 → −0.23 → −0.52 V. The other experimental conditions were the same as those in Figure 2.

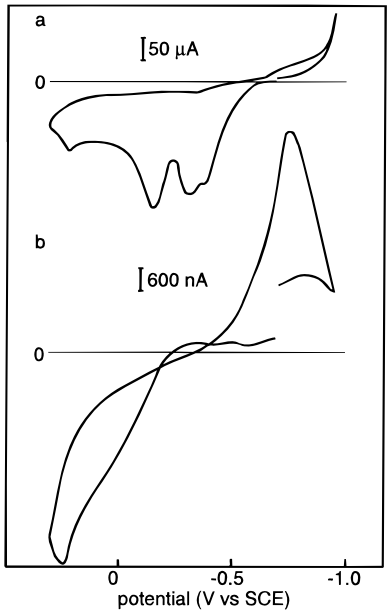

Figure 8. (a) Dark current and (b) photocurrent vs potential curves of a Q-PbS particle layer in a solution containing 2 mM S_2^{2-} and 0.5 M $NaClO_4$. The potential range was between 0.3 and −0.95 V; sweep direction was −0.7 → 0.3 → −0.95 → −0.7 V. The other experimental conditions were the same as those in Figure 2.

anodic photocurrent seen at potentials positive of −0.5 V is due to the photooxidation of $MV^{\bullet+}$ (Scheme 3b). Figure 8 shows the voltammetric curves obtained under illumination in a solution containing sulfide and polysulfide S_x^{2-}. This solution (pH 12.1) was made by stirring 5 mM sulfur and 40 mM Na_2S under argon for about 1 day. Both anodic and cathodic photocurrents were observed in this solution, depending on the bias potential. When the potential was negative of about −0.5 V, the photoassisted reduction of S_2^{2-} to $2S^{2-}$ was the predominant photoprocess (Scheme 3c), and a cathodic photocurrent was observed. When the potential was positive of about −0.4 V, the photoassisted oxidation of S_2^{2-} to S was the main photoprocess (Scheme 3d) and an anodic photocurrent was observed. The results indicate that the net photocurrent can be either cathodic or anodic, depending on the presence of redox species in the solution, the bias potential, and the existence of surface states as shown in Schemes 2 and 3.

Conclusions

A Q-PbS layer on an electrode can be prepared in a self-assembled monolayer on a Au surface. In the dark, Q-PbS particle monolayers with different particle sizes were all oxidized at about 0.25 V vs SCE but were reduced in a range from −1.1 V vs SCE to potentials beyond hydrogen evolution, depending on the size of the particles. Either cathodic or anodic photocurrents were found, depending on the nature of the solution mediator (hole or electron scavenger) and the applied potential.

Acknowledgment. The support of this research by grants from Asahi Chemical Industry Co., Ltd., the National Science Foundation (CHE9423874), and the Robert A. Welch Foundation is gratefully acknowledged. We thank Mark F. Arendt for sputtering the gold on mica.

References and Notes

(1) Gadenne, P.; Yagil, Y.; Deutscher, G. *J. Appl. Phys.* **1989**, *66*, 3019.
(2) Chaudhuri, T. K.; Chatterjes, S. Proc. *Int. Conf. Thermoelectr.* **1992**, *11*, 40.
(3) Hirata, H.; Higashiyama, K. *Bull. Chem. Soc. Jpn.* **1971**, *44*, 2420.
(4) Nair, P. K.; Gomezdaza, O.; Nair, M. T. S. *Adv. Mater. Opt. Electron.* **1992**, *1*, 139.
(5) (a) Cardona, M.; Greenaway, D. L. *Phys. Rev. A* **1964**, *133*, 1685. (b) Catalano, I. M.; Clingolani, A.; Minafra, A. *Phys. Rev. B* **1973**, *8*, 1488. (c) Aspnes, D. E.; Cardona, M. *Phys. Rev.* **1968**, *173*, 714.
(6) Chaudhuri, T. K. *Int. J. Energy Res.* **1992**, *16*, 481.
(7) Takahashi, M.; Ohshima, Y.; Nagata, K.; Furuta, S. *J. Electroanal. Chem.* **1993**, *359*, 281.
(8) Nair, P. K.; Nair, M. T. S. *Semicond. Sci. Technol.* **1989**, *4*, 807.
(9) Davis, A. P.; Huang, C. P. *Langmuir* **1991**, *7*, 803.
(10) Galus, Z. In *Standard Potentials in Aqueous Solution*; Bard, A. J., Parsons, R., Jordan, J., Eds.; Marcel Dekker: New York, 1985.
(11) (a) Hsieh, Y. S.; Huang, C. P. *J. Colloid Interface Sci.* **1989**, *131*, 537. (b) Paul, R. L.; Nicol, M. J.; Diggle, J. W.; Saunders, A. P. *Electrochim. Acta* **1978**, *23*, 625. (c) Gardner, L. R.; Woods, R. *J. Electroanal. Chem. Interfacial Electrochem.* **1979**, *100*, 447.
(12) (a) Gallardo, S.; Gutierres, M.; Henglein, A.; Janata, E. *Ber. Bunsenges. Phys. Chem.* **1989**, *93*, 1080. (b) Rossetti, R.; Hull, R.; Gibson, J. M.; Brus, L. E. *J. Chem. Phys.* **1985**, *83*, 1406. (c) Wang, Y.; Suna, A.; Mahler, W.; Kasowski, R. *J. Chem. Phys.* **1987**, *87*, 7315.
(13) Nenadovic, M. T.; Comor, M. I.; Vasic, V.; Micic, O. I. *J. Phys. Chem.* **1990**, *94*, 6390.
(14) Torimoto, T.; Uchida, H.; Sakata, T.; Mori, H.; Yoneyama, H. *J. Am. Chem. Soc.* **1993**, *115*, 1874.
(15) Torimoto, T.; Sakata, T.; Mori, H.; Yoneyama. H. *J. Phys. Chem.* **1994**, *98*, 3036.
(16) Miyoshi, H.; Yamachika, M.; Yoneyama, H.; Mori, H. *J. Chem. Soc., Faraday Trans.* **1990**, *86*, 815.
(17) Ward, M. D.; White, J. R.; Bard, A. J. *J. Am. Chem. Soc.* **1983**, *105*, 27.
(18) Steigerwald, M. L.; Alivisatos, A. P.; Gibson, J. M.; Harris, T. D.; Kortan, R.; Muller, A. L.; Thayer, A. M.; Duncan, T. M.; Douglass, D. C.; Brus, L. E. *J. Am. Chem. Soc.* **1988**, *100*, 3046.
(19) Ogawa, S.; Fan, F.-R. F.; Bard, A. J. *J. Phys. Chem.* **1995**, *99*, 11182.